MEDEDELINGEN EN VERHANDELINGEN

71

H. C. BIJVOET

A NEW OVERLAY FOR THE DETERMINATION OF THE SURFACE WIND OVER SE FROM SURFACE WEATHER CHARTS

1957

F 2,50

A NEW OVERLAY FOR THE DETERMINATION OF THE SURFACE WIND OVER SEA FROM SURFACE WEATHER CHARTS

H. C. BIJVOET

1957

STAATSDRUKKERIJ- EN UITGEVERIJBEDRIJF/'S-GRAVENHAGE

PUBLIKATIENUMMER: K.N.M.I. 102–71

U.D.C.: 551.501.4:
551.552 (26):
551.542.1 (26)

CONTENTS

VOORWOORD

In 1857 vestigde BUYS BALLOT de aandacht op een verband tussen de wind aan de grond en de luchtdrukverdeling. Vele auteurs hebben sindsdien bijdragen geleverd tot dit onderwerp.

De onderhavige studie, die juist 100 jaar na de ontdekking van de „wet van Buys Ballot" verschijnt, bevat een beschrijving van een diagram, waarmede de wind boven zee op een eenvoudige wijze kan worden afgeleid uit stationaire en niet-stationaire luchtdrukvelden.

Het diagram wordt op het K.N.M.I. gebruikt als een hulpmiddel bij het opstellen van scheepsweerberichten, stormwaarschuwingen en waterstandsverwachtingen.

De Hoofddirecteur van het K.N.M.I.,

C. J. WARNERS

PREFACE

In 1857 BUYS BALLOT drew attention to a relation between the surface wind and the pressure distribution. Many authors have since contributed to this subject. The present study, published just 100 years after the discovery of the „law of Buys Ballot", contains a description of an overlay with which the surface wind over sea can be derived from stationary and non-stationary pressure fields in a simple manner.

The overlay is used in the Royal Netherlands Meteorological Institute as an aid for shipping forecasts, gale warnings and sea level forecasts.

The Director in Chief
Royal Netherlands Meteorological Institute,

C. J. WARNERS

1. INTRODUCTION

1.1 The knowledge of the relation between the pressure distribution and the surface wind over sea has several practical aspects. This knowledge is for instance an essential part of wind forecasting as at present e.g. shipping forecasts, gale warnings, forecasts for sea or swell and warnings for storm surges are mainly based on pressure field forecasts (prebaratics) so far as concerns middle and high latitudes.

But it is also of importance for certain oceanographic research to know as exactly as possible how the surface wind is related to pressure. Owing to the shortage of wind observations, in particular over sea areas outside the main shipping routes, it often occurs that the wind can only be approximated with the aid of the pressure distribution, which in many cases can easier be interpolated over areas with scanty observations.

The principal methods for the determination of the wind *speed* at anemometer elevation from the pressure field on M.S.L. can be summarized as follows.

1.1.1 If the pressure field is quasi stationary and when the isobars are approximately straight the wind speed can be determined with the formula

$$v = c\frac{G}{f} = cv_g \tag{1}$$

in which v denotes the wind velocity, c the friction factor, f the coriolis parameter, G the absolute value of the horizontal pressure gradient and v_g the geostrophic wind speed. [1])

1.1.2 When the pressure field is quasi stationary and the isobars curved the windspeed can be approximated by the equation

$$v = c\left\{\tfrac{1}{2}rf\left(1 - \sqrt{1 - \frac{4G}{f^2 r}}\right)\right\} = cv_{gr} \tag{2}$$

In this formula represents r the curvature of the trajectory of an individual unit of air and v_{gr} the gradient wind speed. For the curvature r can be taken the curvature of the isobar (r_i) through the point concerned.

1.1.3 When the pressure distribution changes in time the wind can be approximated by [4,3]

$$v = c\left|\vec{v}_{gr} + \frac{1}{f^2}\frac{\partial \vec{G}}{\partial t}\right| \tag{3}$$

---

[1]) A complete description of the symbols used is given in section 7.

1.1.4 When the pressure field is non-stationary but the pressure patterns are moving practically without deformation Eq. (2) can be applied as well but it is not allowed to use r_i instead of r. The curvature r can be determined for instance with the method described in [10] or with the formula [8]:

$$\frac{1}{r} = \frac{1}{r_i}\left(1 - f\frac{C}{G}\cos\psi\right) \tag{4}$$

where C denotes the velocity with which the pressure pattern is moving and ψ the angle between $\vec{C}$ and $\vec{v}_g$.

1.2 There exists much uncertainty about the accuracy of the above mentioned methods. In the literature different values can be found for the friction factor as a consequence of differences in opinion about the factors on which c depends. Moreover none of the methods holds in all cases in view of the theory on which the equations are based. The relations are all approximations and the accuracy depends on the extent to which the pressure field satisfies certain conditions. These conditions are expressed by terms like „quasi-stationary", „approximately straight isobars" and „stiff moving pressure patterns". The application of the equation (3) is also limited [9].

From a practical point of view it is of importance to know the order of magnitude of the differences between the results obtained by application of the various methods in comparison with the order of magnitude of errors which have to be imputed to inexactitudes of the analysis of the pressure distribution. For the determination of the surface wind from prebaratics for more than 12 hours in future and from pressure analyses (baratics) of sea areas with scanty observations it makes no sense to use other relations between wind and pressure than the simple Eq. (1). But what rules must be followed if the pressure distribution is known more precisely? It is generally assumed that for stationary pressure fields with *curved* isobars Eq. (2) gives better results than Eq. (1). Does this also apply to moving and developing pressure patterns?

There are further cases where the pressure distribution in space is known with a rather high degree of exactness while the local pressure changes (pressure tendencies) are practically unknown so that Eq. (3) cannot be applied. What errors can be expected when Eq. (2) is used instead of Eq. (3) and are these errors of such an order of magnitude that they must be kept in mind for safety's sake when issuing „warnings"?

1.3 This contribution deals with the mentioned problems. To that the relation between surface wind and pressure has been subjected once more to a further consideration. With the aid of the obtained knowledge a new and rather simple diagram for the determination of the wind speed at about 10 meters

above the sea's surface from stationary and non-stationary pressure fields could be constructed. The diagram used as overlay on weather maps enables one in each separate case to oversee directly to which parameters special attention has to be paid for the most accurate possible determination of wind velocity.

2. THE RELATION BETWEEN SURFACE WIND AND PRESSURE IN PARTICULAR OVER SEA

2.1 The relation between wind and pressure in the friction layer of the atmosphere (the layer from the earth's surface to a height of about 800 meters) can be expressed by the simplified equation of motion:

$$\frac{d\vec{v}}{dt} = \vec{G} + f\vec{v} \times \vec{k} + \vec{R} \tag{5}$$

In this equation $\vec{G}$ denotes the gradient force, $f\vec{v} \times \vec{k}$ the Coriolis force and $\vec{R}$ the friction force, all per unit of mass.

We consider as a first step a non-accelerated motion. Under that condition we may write

$$\vec{G} + f\vec{v} \times \vec{k} + \vec{R} = 0 \tag{6}$$

This balance of forces is shown in fig. 1.

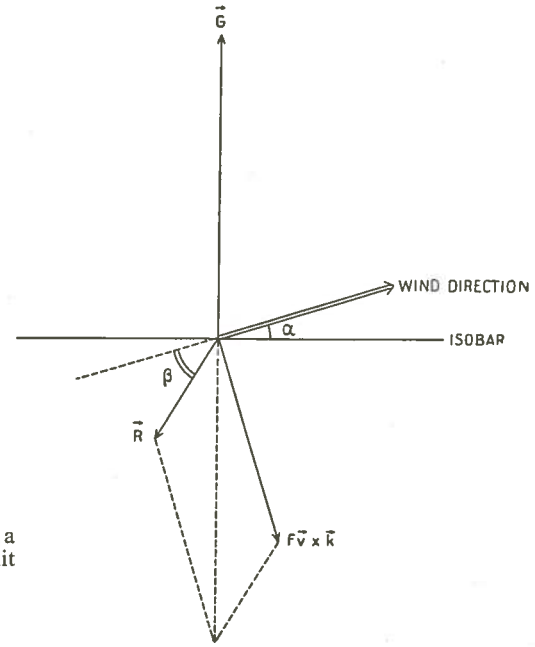

FIG. 1. Balance of forces acting on a non-accelerated moving unit of air.

It is generally assumed that R is proportional to v [1,6]. With the aid of fig. 1 we can then derive:

$$tg\,\beta = \operatorname{cotg}\alpha - c\,.\,\operatorname{cosec}\alpha \tag{7}$$

and

$$v = c\,\frac{G}{f} \tag{8}$$

where β indicates the angle between $\vec{R}$ and $-\vec{v}$ and α the angle between $\vec{v}$ and $\vec{v}_g$.

Further can be derived

$$R = \varkappa f v \tag{9}$$

in which

$$\varkappa = \sqrt{\frac{1}{c^2} - \frac{2\cos\alpha}{c} + 1} \tag{10}$$

The coefficient $\varkappa$ is usually denoted as the friction coefficient.

2.2 We shall now try to inquire on which factors c and α are depending. The „Austausch" theory procures the relation

$$\vec{R} = \frac{\partial}{\partial z}\,\frac{A}{\varrho}\,\frac{\partial \vec{v}}{\partial z} \tag{11}$$

in which A indicates the „Austausch" coefficient and ϱ the air density. For a non-accelerated air motion it follows from Eqs. (6) and (11):

$$\vec{G} + f\vec{v} \times \vec{k} + \frac{\partial}{\partial z}\,\frac{A}{\varrho}\,\frac{\partial \vec{v}}{\partial z} = 0 \tag{12}$$

Assuming that $\vec{G}$ and A/ϱ are constant within the friction layer, $v = f^{-1}\,\vec{G} \times \vec{k} \neq 0$ above the friction layer and $v = 0$ at the earth's surface, the following relations can be derived from Eq. (12) (See e.g. [7], theory of the EKMAN's spiral)

$$v = \frac{G}{f}\sqrt{1 - 2e^{-\lambda z}\cos\lambda z + e^{-2\lambda z}} \tag{13}$$

and

$$R = fv\,\frac{e^{-\lambda z}}{\sqrt{1 - 2e^{-\lambda z}\cos\lambda z + e^{-2\lambda z}}} \tag{14}$$

where $\lambda = \dfrac{f\varrho}{2A}$

Comparing the Eqs. (8) and (9) with (13) and (14) it appears that for a certain height, latitude and density, c and $\varkappa$ only depend on the „Austausch" coefficient.

2.3 The determination of the „Austausch" coefficient in the friction layer over sea is limited to incidentical investigations. The data show that A in the lowest layers of the atmosphere mainly depends on the stability of the air. The difference between the air temperature (T) and the temperature of the sea's surface (T_s) can be used as a measure of stability.

Form data collected and investigated by BLEEKER and VERPLOEGH it appears possible to determine c and $\varkappa$ as a function of $T—T_s$ and the wind velocity which can be used as a measure of the roughness of the surface of the sea.

BLEEKER [2] has investigated the relation between c and $T—T_s$ for quasi-stationary pressure patterns with straight isobars and with the aid of wind records from the light-vessel Noord-Hinder (52N, 3E). The relation between c and $T—T_s$ averaged over all wind velocities is shown in fig. 2.

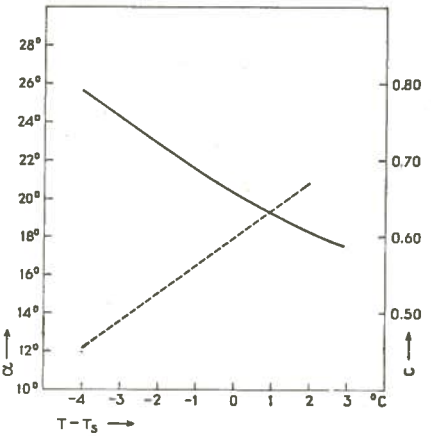

FIG. 2.
The relation between c and $T—T_S$ (—) and between α and $T—T_S$ (------).

VERPLOEGH [12] has determined the angle between v and v_g for quasi-stationary pressure distributions with straight isobars using observations of Dutch ships on the North Atlantic. The results of this investigation show that α is related to $T—T_s$. A relation between α and v is uncertain but if there exists a dependence it must be considered as an effect of second order.

Form the data of VERPLOEGH we assume as first approximation α proportional to $T—T_s$ inside the interval $T—T_s = —4°C$ and $T—T_s = 2°C$ and for wind velocities < 25 m.p.s. We assume further from [12] $\alpha = 15°$ for $T—T_s = —2.0°C$ and $\alpha = 20°$ for $T—T_s = 1.4°C$. The relation between α and $T—T_s$ settled in this way is shown in fig. 2.

VERPLOEGH [11] has investigated moreover the relation between c and v with the aid of observations from Dutch ships on the North Atlantic in the vicinity of 50° latitude. On the basis of these data and the investigation [2] it may be assumed that c mainly depends on $T—T_s$ and further that c is practically independent of v for windvelocities < 25 m.p.s.

Using the relation given in fig. 2 the values for β and $\varkappa$ have been computed with the Eqs. (7) and (8) and represented in fig. 3.

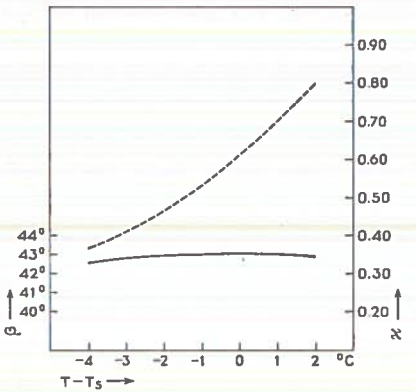

FIG. 3.
The relation between $\varkappa$ and $T—T_s$ (------) and between β and $T—T_s$ (——).

2.4 The relation between surface wind and pressure derived in the foregoing sections is restricted to non-accelerated air motions. For an extension of the theory to accelerated air motions and non-stationary pressure distributions we make use of the investigations published by HESSELBERG and SVERDRUP [5, 6].

To that we write Eq. (5) in the form:

$$\vec{v} = \frac{1}{f}\left(\vec{G} + \vec{R} - \frac{\partial \vec{v}}{\partial t}\right) \times \vec{k} \tag{15}$$

This equation can be approximated by

$$\vec{v} = \frac{1}{f}(\vec{G}+\vec{R}) \times k + \frac{1}{f^2}\frac{d}{dt}(\vec{G}+\vec{R}) - \frac{1}{f^3}\frac{d}{dt}(\vec{G}+\vec{R}) \times \vec{k} + \ldots . \tag{16}$$

According to HESSELBERG the series (16) converges rapidly so that

$$\vec{v} = \frac{1}{f}(\vec{G}+\vec{R}) \times \vec{k} + \frac{1}{f^2}\frac{d}{dt}(\vec{G}+\vec{R}) \tag{17}$$

may be considered as a useful relation between wind and pressure.

HESSELBERG and SVERDRUP have shown further that for non-stationary pressure patterns the values of β and $\varkappa$ appear practically equal to the values derived from stationary pressure fields with non-accelerated air motion. This experience implies that the acceleration is mainly a consequence of changes of the gradient force which acts on an air particle.

When for a certain value of $T—T_s$ the angle β and the friction coefficient are

constants and using a horizontal rectangular coordinate system x, y the solution of Eq. (17) may be written

$$v_x = \frac{\frac{a_1}{f} G_y + \frac{a_2}{f} G_x - \frac{a_3}{f^2}\left(\frac{\partial G_y}{\partial t} + v_y \frac{\partial G_y}{\partial y}\right) - \frac{a_4}{f^2}\left(\frac{\partial G_x}{\partial t} + v_y \frac{\partial G_x}{\partial y}\right)}{1 + \frac{a_3}{f^2}\frac{\partial G_y}{\partial x} + \frac{a_4}{f^2}\frac{\partial G_x}{\partial x}} \tag{18a}$$

and

$$v_y = \frac{\frac{a_2}{f} G_y - \frac{a_1}{f} G_x - \frac{a_4}{f^2}\left(\frac{\partial G_y}{\partial t} + v_x \frac{\partial G_y}{\partial x}\right) + \frac{a_3}{f^2}\left(\frac{\partial G_x}{\partial t} + v_x \frac{\partial G_x}{\partial x}\right)}{1 + \frac{a_4}{f^2}\frac{\partial G_y}{\partial y} - \frac{a_3}{f^2}\frac{\partial G_x}{\partial y}} \tag{18b}$$

In the Eqs. (18a) and (18b) represent:

$$a_1 = \frac{1 + \varkappa \,.\, \sin\beta}{(\varkappa \,.\, \cos\beta)^2 + (1+\varkappa \,.\, \sin\beta)^2}$$

$$a_2 = \frac{\varkappa \,.\, \cos\beta}{(\varkappa \,.\, \cos\beta)^2 + (1+\varkappa \,.\, \sin\beta)^2}$$

$$a_3 = \frac{2\,(\varkappa \,.\, \cos\beta)\,(1+\varkappa \,.\, \sin\beta)}{\{(\varkappa \,.\, \cos\beta)^2 + (1+\varkappa \,.\, \sin\beta)^2\}^2}$$

$$a_4 = \frac{(\varkappa \,.\, \cos\beta)^2 - (1+\varkappa \,.\, \sin\beta)^2}{\{(\varkappa \,.\, \cos\beta)^2 + (1+\varkappa \,.\, \sin\beta)^2\}^2}$$

The coefficients a_1, a_2, a_3 and a_4 can be computed for different values of $T—T_s$ with the values of $\varkappa$ and β as shown in fig. 3. The results are given in table 1.

TABLE 1. *Coefficients a_1, a_2, a_3 and a_4*

$T—T_s$	—4	—2	0	+2°C
a_1	0,77	0,71	0,64	0,58
a_2	0,16	0,18	0,20	0,21
a_3	0,25	0,26	0,26	0,25
a_4	—0,56	—0,48	—0,38	—0,29

If we fix the y-axis in the direction of $\vec{G}$ then we may write $G_x = 0$ and

$$\frac{\partial G_x}{\partial x} = \frac{G_y}{r_i} = \frac{f v_g}{r_i} \tag{19}$$

Furthermore can be written if f is considered as a constant

$$\frac{\partial G_y}{\partial y} = f \frac{\partial v_g}{\partial y} \tag{20}$$

Resuming it may now be said that according to the Eqs. (18), (19) and (20) the wind at 10 meters above the sea's surface depends on:

1) the geostrophic wind (G_y and $\partial G_x/\partial x$);
2) the horizontal shear of the geostrophic wind ($\partial G_y/\partial y$);
3) the curvature of the isobars ($\partial G_x/\partial x$);
4) the difluence of the isobars ($\partial G_y/\partial x$ and $\partial G_x/\partial y$);
5) the isallobaric gradient ($\partial G_x/\partial t$ and $\partial G_y/\partial t$);
6) the stability of the air (T—T_s);
7) the latitude (f).

3. A COMPARISON OF THE DIFFERENT METHODS FOR THE DETERMINATION OF THE WIND

3.1 For practical purposes it is desirable to know the differences between the results obtained by application of Eq. (18) and the easier to handle Eqs. (1), (2), (3) and (4). It appeared impossible to collect sufficient data for an empirical investigation, because such an investigation requires a long series of wind records of a point on sea around which the pressure distribution in space and time is known with a high degree of accuracy. From a theoretical point of view, however, we may assume that Eq. (18) approximates the relation between wind and pressure more precisely than the other equations. Further it is known from experience that the surface wind only reaches the geostrophic value under exceptionally unstable conditions. It will be shown in the following sections that in a number of by no means exceptional cases, the application of the Eqs. (2) and (3) leads to values > 1 for the ratio v/v_g, while the corresponding values derived from Eq. (18) remain more realistic.

On the whole there are sufficient reasons to consider the differences between the results of Eq. (18) on the one hand and the Eqs. (1), (2), (3) and (4) on the other hand, as a relative measure for the accuracy of the methods for the determination of the wind mentioned in the introduction.

3.2 For a comparison of the different methods the equations have to be modified so that the same parameters appear in the relations. Therefore we substitute Eq. (19) into (2) and assume $r = r_i$. We can then write

$$\frac{v}{v_g} = \frac{1}{2} \frac{cf^2}{\partial G_x/\partial x} \left(1 - \sqrt{1 - \frac{4 \partial G_x/\partial x}{f^2}} \right) \tag{21}$$

The ratio v/v_g in this equation depends on c, f and $\partial G_x/\partial x$.

For a stationary pressure distribution ($\partial G_x/\partial t = \partial G_y/\partial t = 0$) with equidistant isobars ($\partial G_y/\partial x = \partial G_x/\partial y = \partial G_y/\partial y = 0$) the ratio v/v_g also depends on c, f and $\partial G_x/\partial x$ according to Eq. (18).

TABLE 2. *v/v_g computed with Eq. (18) and Eq. (21) for 55° latitude*

$\partial G_x/\partial x$	$T-T_s = -4°C$, $c = 0{,}79$		$T-T_s = +2°C$, $c = 0{,}61$	
	v/v_g computed with		v/v_g computed with	
	(18)	(21)	(18)	(21)
-8×10^{-8} sec^{-2}	0,23	0,27	0,24	0,21
-6	0,24	0,30	0,28	0,23
-4	0,30	0,36	0,33	0,28
-2	0,43	0,48	0,41	0,38
0	0,79	0,79 [1]	0,61	0,61 [1]
0,3	0,91	1,26	0,67	0,97
1	1,34	— [2]	0,79	— [2]

[1] Limit for $\partial G_x/\partial x \to 0$.
[2] For $\partial G_x/\partial x > \frac{1}{4} f^2$ Eq. (21) gives no solution.

Table 2 shows the corresponding values for v/v_g computed with the Eqs. (18) and (21). We see from table 2 that the differences remain small for cyclonic curved isobars ($\partial G_x/\partial x < 0$) but considerable deviations appear for anticyclonic curvature ($\partial G_x/\partial x > 0$). For 55° latitude ($f = 12 \times 10^{-4}$ sec^{-1}), $v_g = 15$ m/sec and a radius of curvature of the isobar = 600 km we find with the aid of Eq. (19) $\partial G_x/\partial x = 0.3 \times 10^{-8}$ sec^{-2}. We see now from table 2 that for $\partial G_x/\partial x = 0.3 \times 10^{-8}$ sec^{-2} and $T-T_s = 2°C$ (stable atmosphere) $v = 0.67\ v_g$ according to Eq. (18) but $v = 0.97\ v_g$ if Eq. (2) is used. For an unstable atmosphere ($T-T_s = -4°C$) Eq. (2) leads to $v = 1.26\ v_g$. These improbable results obtained by application of Eq. (2) favour the reliability of Eq. (18) which under the same conditions, gives more realistic values.

3.3 In the foregoing section it has been supposed that the isobars are equidistant. We will now trace the effect of horizontal geostrophic windshear ($\partial G_y/\partial y$) and difluence of the flow ($\partial G_y/\partial x = \partial G_x/\partial y$) on the wind speed. Table 3 gives the ratio v/v_g as a function of $\partial G_x/\partial x$ and $\partial G_y/\partial y$ for a stationary pressure distribution without difluence. Table 4 shows v/v_g as a function of $\partial G_x/\partial x$ and $\partial G_y/\partial x$ for a stationary pressure field without geostrophic windshear.

TABLE 3. *v/v_g computed with Eq. (18) for 55° latitude*

$\partial G_y/\partial y$	$T-T_s = -4°C$, $c = 0{,}79$			$T-T_s = +2°C$, $c = 0{,}61$		
	−1	0	+1	−1	0	+1
	$\times 10^{-8}$ sec^{-2}			$\times 10^{-8}$ sec^{-2}		
$\partial G_x/\partial x$						
-4×10^{-8} sec^{-2}	0,29	0,30	0,31	0,32	0,33	0,33
−2	0,43	0,43	0,43	0,42	0,41	0,41
0	0,80	0,79	0,78	0,63	0,61	0,60
0,3	0,91	0,91	0,88	0,68	0,67	0,63
1	1,37	1,34	1,24	0,83	0,79	0,76

TABLE 4. *v/v_g computed with Eq. (18) for 55° latitude*

$\partial G_y/\partial x$	$T-T_s = -4°C$, $c = 0{,}79$			$T-T_s = +2°C$, $c = 0{,}61$		
	−1	0	+1	−1	0	+1
	$\times 10^{-8}$ sec^{-2}			$\times 10^{-8}$ sec^{-2}		
$\partial G_x/\partial x$						
-4×10^{-8} sec^{-2}	0,37	0,30	0,30	0,36	0,33	0,30
−2	0,52	0,43	0,46	0,47	0,41	0,42
0	1,01	0,79	0,98	0,69	0,61	0,65
0,3	1,17	0,91	1,12	0,74	0,67	0,72
1	1,83	1,34	1,63	0,88	0,79	0,88

From table 3 it can be seen that the influence of the geostrophic windshear is small even when $\partial G_y/\partial y$ reaches the extreme values -10^{-8} and $+10^{-8}$ sec^{-2} corresponding with a geostrophic shear of 8 m/sec/100 km. The effect of difluence is much greater. However the values in table 4 are of little more than academic interest because *stationary* and strong difluent or confluent flows never occur.

3.4 Among the methods for the determination of the surface wind from *non*-stationary pressure fields the method mentioned in section **1.1.4** is the simplyest one. The application is limited because stiff moving pressure patterns do not frequently occur. The method appears most suitable for the determination of the wind in the axis of moving troughs and ridges.

Substituting Eq. (19) into Eq. (4) and taking into account the orientation of the coordinates as mentioned in section 2.4 we can derive

$$\frac{1}{r} = \frac{\partial G_x/\partial x}{f v_g}\left(1 - \frac{C_x}{v_g}\right) \tag{22}$$

Substitution of Eq. (22) into Eq. (2) leads to

$$\frac{v}{v_g} = \frac{1}{2}\frac{cf^2}{\dfrac{\partial G_x}{\partial x}\left(1 - \dfrac{C_x}{v_g}\right)}\left\{1 - \sqrt{1 - 4\frac{\partial G_x/\partial x}{f^2}\left(1 - \frac{C_x}{v_g}\right)}\right\} \tag{23}$$

In this equation the ratio v/v_g depends on c, f, $\partial G_x/\partial x$ and C_x/v_g. A similar relation with the same parameters can be derived from Eq. (18).

Supposing the isobars equidistant ($\partial G_y/\partial x = \partial G_y/\partial y = 0$) and no deformation of the pressure pattern ($\partial G_y/\partial t = 0$) and using the relation

$$\frac{\partial G_x}{\partial t} = - C_x \frac{\partial G_x}{\partial x} \tag{24}$$

it follows from Eq. (18)

$$\frac{v_x}{v_g} = \frac{a_1 + a_4 f^{-2}\,(\partial G_x/\partial x)\,(C_x/v_g)}{1 + a_4 f^{-2}\,(\partial G_x/\partial x)}$$

and (25)

$$\frac{v_y}{v_g} = a_2 - a_3 f^{-2}\,(\partial G_x/\partial x)\,(C_x/v_g - v_x/v_g)$$

TABLE 5. *v/v_g computed with Eq. (23) for 55° latitude.*
$T - T_s = -2°C$ ($c = 0{,}72$)

C_x/v_g	—0,4	—0,2	0	0,2	0,4	0,6	0,8	1,0
$\partial G_x/\partial x$								
-4×10^{-8} sec^{-2}	0,29	0,31	0,33	0,37	0,42	0,50	0,59	0,72
—2	0,39	0,42	0,45	0,50	0,54	0,59	0,65	0,72
—1	0,52	0,54	0,57	0,59	0,62	0,65	0,68	0,72
0,3	—[1]	1,44	1,17	0,91	0,86	0,80	0,76	0,72
1	—	—	—	—	—	—	0,89	0,72

[1] — Eq. (23) gives no solution.

Table 5 shows the values for v/v_g computed with Eq. (23) as a function of $\partial G_x/\partial x$ and C_x/v_g. In the column for $C_x/v_g = 1.0$ we find $v/v_g = c$ for all

TABLE 6. *v/v_g computed with Eq. (25) for 55° latitude.*
$T—T_S = —2°C$ ($c = 0{,}72$)

C_x/v_g	—0,4	—0,2	0	0,2	0,4	0,6	0,8	1,0
$\partial G_x/\partial x$								
-4×10^{-8} sec^{-2}	0,23	0,25	0,32	0,43	0,56	0,67	0,79	0,92
—2	0,32	0,37	0,43	0,51	0,63	0,70	0,77	0,86
—1	0,46	0,47	0,50	0,56	0,65	0,72	0,73	0,81
0,3	0,85	0,86	0,85	0,83	0,81	0,80	0,77	0,71
1	1,31	1,24	1,08	0,99	0,91	0,84	0,74	0,58

values of $\partial G_x/\partial x$. This cannot be correct. When the speed of a stiff moving trough is greater than the windspeed of an air particle in the axis (which is the case with $C_x = v_g$) the trajectory of that unit of air has an anticyclonic curvature [10]. That implies that v must be greater than cv_g. On the other hand if a ridge is moving faster than the wind in the axis the trajectory of an air particle in the axis has a cyclonic curvature which means that v must be smaller than cv_g. The computations based on Eq. (25) are in agreement with that as can be seen from table 6. For $C_x/v_g = 1.0$ the ratio v/v_g is greater than c if $\partial G_x/\partial x < 0$ (cyclonic curvature of the isobars) and $v/v_g < c$ when $\partial G_x/\partial x > 0$ (anticyclonic curvature). This result is again in favour of the accuracy of Eq. (18) from which Eq. (25) has been derived.

3.5 If a pressure distribution is non-stationary there will mostly blow a wind different from the wind which would blow if the same pressure pattern was stationary. We denote the vector difference by $\vec{v}'$. The method mentioned in section 1.1.3 is based on the assumption that in the free atmosphere $\vec{v}'$ can be approximated by

$$\vec{v}' = \frac{1}{f^2} \frac{\partial \vec{G}}{\partial t} \tag{26}$$

This relation has led to the introduction of the notion „isallobaric wind". PHILLIPS [9] has drawn attention to the fact that $\vec{v}'$ not only depends on $\partial G/\partial t$ but moreover on $\partial G_x/\partial x$, $\partial G_y/\partial y$ and $\partial G_y/\partial x$ as can also be seen from Eq. (18).

To compare the results of Eq. (18) with those obtained from Eq. (3) a number of realistic models of non-stationary pressure distributions containing all the characteristic features of the principal pressure patterns has been investigated. A review of the models considered is given on the next page.

Review of investigated models

Model number	Pressure pattern	Developments resulting from the assumed distribution of $\partial p/\partial t$	Stability of the air $(T—T_s)$ °C
1	Non-occluded wave disturbance with a closed pressure centre at the top of the warm sector	Wave centre moving 90 km/h in the direction of the warm sector isobars. Pressure in the centre remains stationary	In the warm sector +2°. Outside the warm sector —2°
2	As nr. 1	As nr. 1 but depression deepening 1 mb/hour	As nr. 1
3	Part of an occluded depression	Front moving with the velocity of the wind component perpendicularly to the front in the post frontal air	Pre-frontal +2° Post-frontal —2°
4	Pronounced trough	Trough moving 36 km/h in the direction perpendicularly to the trough axis. No deformation of the isobar pattern	—4°
5	As nr. 4	As nr. 4 but trough moving 90 km/hour	—4°
6	As nr. 4	As nr. 5	+2°
7	As nr. 4	As nr. 5 but trough filling	—4°
8	As nr. 4	As nr. 5 but trough deepening	—4°
9	Anticyclone	Centre of the anticyclone moving 30 km/hour	0°
10	Ridge of high pressure	Ridge moving 36 km/h in the direction perpendicularly to the axis; ridge intensifying	0°

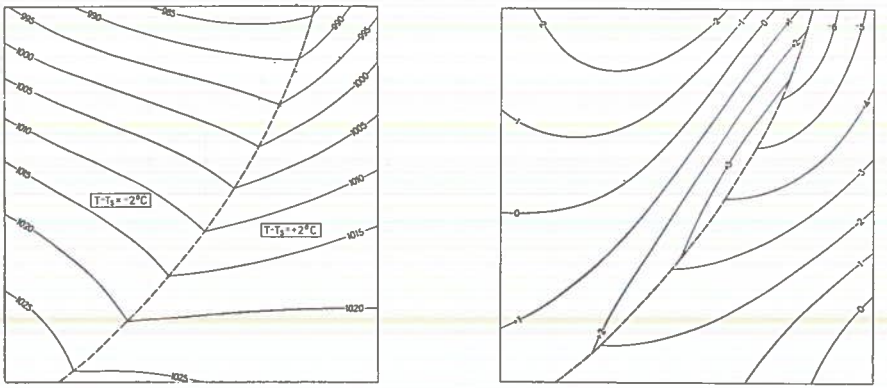

FIG. 4. Model of a part of an occluded depression.

a. —— isobars (mb); ------ front. *b.* —— $\partial p/\partial t$ (mb/3 hours); ------ front.

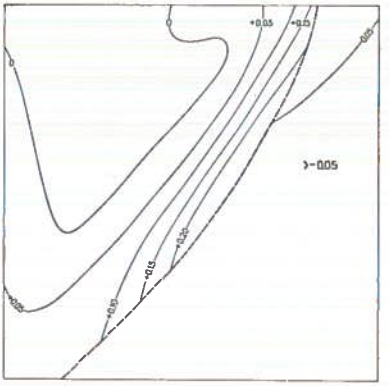

FIG. 5. Distribution of v/v_g computed with Eq. (18) minus v/v_g computed with Eq. (3) ——; front ------.

Fig. 4 shows as example model 3 representing a part of an occluded depression with the assumed field of $\partial p/\partial t$. Fig. 5 indicates the distribution of the differences between v/v_g computed with Eq. (18) and v/v_g derived from Eq. (3). Fig. 6 and 7 show the results when applying the Eqs. (1) and (2) on this non-stationary pressure field. Conformable computations have been carried out for all other models.

Next the square of the areas where the differences for v/v_g are smaller than —0.10 and greater than +0.10 have been determined. The results are given in table 7. From this table it can be seen that the considered methods show

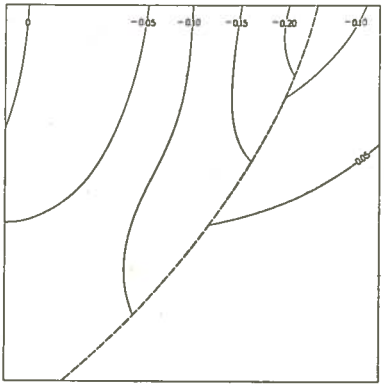

FIG. 6. Distribution of v/v_g computed with Eq. (18) minus v/v_g computed with Eq. (1) ——; front ------.

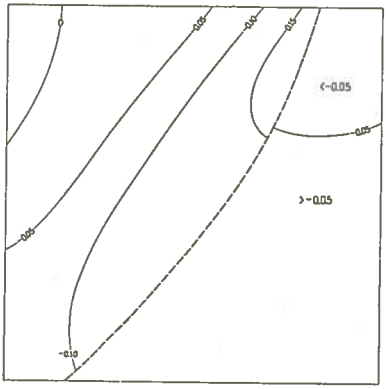

FIG. 7. Distribution of v/v_g computed with Eq. (18) minus v/v_g computed with Eq. (2).

in mean no great differences but pronounced deviations occur for the individual models. It appears again that in certain areas of some models v/v_g computed with Eq. (3) exceeds the value 1 while the corresponding values for v/v_g derived from Eq. (18) remain acceptable.

TABLE 7. *Part (%) of the model square where the differences between v/v_g computed with Eq.* (18) *and other equations are smaller than* —0,10 *and greater than* +0,10

Model number	v/v_g computed with Eq. (18) minus v/v_g computed with Eq. (1)			v/v_g computed with Eq. (18) minus v/v_g computed with Eq. (2)			v/v_g computed with Eq. (18) minus v/v_g computed with Eq. (3)		
	difference			difference			difference		
	<—0,10	>0,10	total	<—0,10	>0,10	total	<—0,10	>0,10	total
1	10	3	13	12	3	15	6	1	7
2	9	6	15	14	6	20	2	1	3
3	20	0	20	21	0	21	0	9	9
4	61	0	61	0	2	2	19	0	19
5	17	3	20	0	16	16	41	0	41
6	0	4	4	0	14	14	13	0	13
7	32	1	33	0	9	9	44	0	44
8	28	5	33	2	22	24	72	0	72
9	0	16	16	33	0	33	23	3	26
10	0	9	9	48	0	48	12	6	18

4. THE CONSTRUCTION OF AN OVERLAY FOR THE DETERMINATION OF THE SURFACE WIND OVER SEA

4.1 We have seen in section 3 that in a number of cases the differences between the results of Eq. (18) and the methods mentioned in the introduction can hardly be neglected but on the other hand the application of Eq. (18) requires extensive computation which is a drawback to employing it in practice.

However it appears possible to simplify Eq. (18) without an essential decrease of accuracy.

If the positive y-axis coincides with $\vec{G}$ we can derive from Eq. (18) using the relation $v = v_x \sec \alpha$

$$v = \frac{\left\{\frac{a_1}{f} G_y - \frac{a_3}{f^2}\frac{\partial G_y}{\partial t} - \frac{a_4}{f^2}\frac{\partial G_x}{\partial t}\right\} \sec \alpha}{1 + \frac{a_4}{f^2}\frac{\partial G_x}{\partial x} + \frac{a_3}{f^2}\frac{\partial G_y}{\partial y} tg\alpha + \left(\frac{a_3}{f^2} + \frac{a_4}{f^2} tg\,\alpha\right)\frac{\partial G_y}{\partial x}} \tag{27}$$

Taking into account the signs and magnitude of a_3, a_4 and $tg\ \alpha$ we now reduce Eq. (27) to

$$v = \frac{\left\{\frac{a_1}{f} G_y - \frac{a_3}{f^2}\frac{\partial G_y}{\partial t} - \frac{a_4}{f^2}\frac{\partial G_x}{\partial t}\right\} \sec \alpha}{1 + \frac{a_4}{f^2}\frac{\partial G_x}{\partial x}} \tag{28}$$

TABLE 8. *Part (%) of the model square where the differences between v/v_g computed with Eq. (18) and Eq. (28) are smaller than —0,10 and greater than +0,10*

Model number	v/v_g computed with Eq. (18) minus v/v_g computed with Eq. (28)		
	difference		
	$<$—0,10	$>$0,10	total
1	0	0	0
2	0	0	0
3	0	0	0
4	0	0	0
5	0	0	0
6	0	3	3
7	0	0	0
8	0	1	1
9	6	0	6
10	9	0	9

To trace the reduction of accuracy of the approximation (28) we have computed again the ratio v/v_g for all models mentioned in section 3.5 using for α the values given in fig. 2. The results of this inquiry are represented in table 8. It appears that the differences between the computations based on Eq. (18) and Eq. (28) remain small in almost all cases.

4.2 For the determination of the surface wind over sea from surface weather maps a relatively simple diagram can now be constructed with the aid of Eq. (28). We introduce the following notations,

$$v_s \equiv \frac{a_1}{f} G_y \sec\alpha, \quad v_i \equiv -\left\{\frac{a_3}{f^2}\frac{\partial G_y}{\partial t} + \frac{a_4}{f^2}\frac{\partial G_x}{\partial t}\right\}\sec\alpha$$

and

$$q \equiv 1 + \frac{a_4}{f^2}\frac{\partial G_x}{\partial x}.$$

Eq. (28) can be written then in the form

$$v = \frac{v_s + v_i}{q} \tag{29}$$

The wind speed v can now be represented in a diagram as a function of $v_s + v_i$ and q by means of isotacs.
We make use further of the following relations:

$$v_s(x, y) = -\frac{a_1}{\varrho f}\frac{p(x, y + \frac{1}{2}\delta_1) - p(x, y - \frac{1}{2}\delta_1)}{\delta_1}\sec\alpha =$$

$$= -\frac{a_1}{\varrho f}\frac{p(x, y) - p(x, y - \delta_1)}{\delta_1}\sec\alpha \tag{30}$$

because it is assumed that $\partial G_y/\partial y = 0$.
Next we write

$$q(x, y) = 1 - \frac{a_4}{\varrho f^2}\frac{p(x + \delta_2, y) + p(x - \delta_2, y) - 2p(x, y)}{{\delta_2}^2} =$$

$$= 1 - \frac{a_4}{\varrho f^2}\frac{2p(x + \delta_2, y) - 2p(x, y)}{{\delta_2}^2} \tag{31}$$

since it is assumed that $\partial G_y/\partial x = 0$, which means that $p(x + \delta_2, y) = p(x - \delta_2, y)$ with the exception of a flexion point in which case $q = 1$.
Finally we may write

$$v_i = \frac{a_3}{\varrho f^2}\left\{\frac{\partial p/\partial t\,(x, y + \frac{1}{2}\delta_2) - \partial p/\partial t\,(x, y - \frac{1}{2}\delta_3)}{\delta_3} + \right.$$

$$\left. + \frac{\partial p/\partial t\,(x + \frac{1}{2}\delta_4, y) - \partial p/\partial t)\,x - \frac{1}{2}\delta_4, y)}{(a_3/a_4)\,\delta_4}\right\}\sec\alpha \tag{32}$$

If taking $\delta_4 = \frac{a_4}{a_3}\delta_3$ we can derive from Eq. (32)

$$v_i = \frac{2a_3}{\varrho f^2}\left\{\frac{\partial p/\partial t\,(x + \frac{1}{4}\frac{a_4}{a_3}\delta_3,\, y + \frac{1}{4}\delta_3) - \partial p/\partial t\,(x - \frac{1}{4}\frac{a_4}{a_3}\delta_3,\, y - \frac{1}{4}\delta_3)}{\delta_3}\right\}\sec\alpha. \quad (33)$$

We fix continually $p\,(x, y) - p\,(x, y - \delta_1) = p\,(x + \delta_2, y) - p\,(x, y) = 5$ mb for cyclonic curved isobars and —5mb if the curvature of the isobars is anticyclonic. For a certain value of ϱ, f and $T—T_s$, v_s can now be considered as a function of δ_1, v_i as a function of δ_3 and q as a function of δ_2, but this relation is different for cyclonic and anticyclonic curvatures of the isobars.

Now plot δ_2 along the horizontal axis of a diagram and δ_1 along the vertical axis. Since a certain value of δ_1 corresponds with a certain value of v_s a wind speed scale can be added along the vertical axis. Further take the scale of δ_1

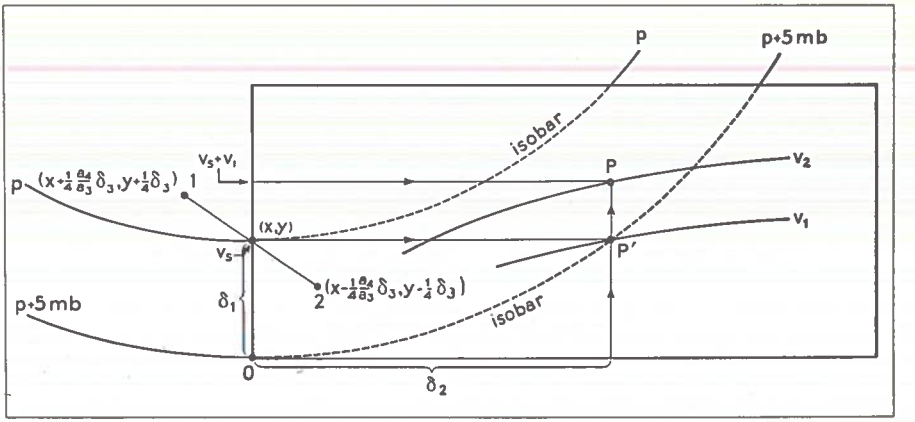

FIG. 8. Schematic representation of the relation between δ_2, v_s and v (——) and directions for the determination of the wind from a weather map (cyclonic curvature of the isobars).

and δ_2 equal to the scale of the weather chart. The determination of the wind speed with the aid of this diagram is rather simple as can be seen from an example (fig. 8).

Suppose we want to know the wind speed at 10 m above the sea's surface at a point (x, y). Use a transparent diagram as overlay on an analysed surface weathermap. Put the left side of the overlay perpendicularly to the isobar p through (x, y) and the origin O on the isobar $p + 5$ mb as indicated in fig. 8. The value of δ_1 corresponds with a certain value of v_s and δ_2 corresponds with a certain value of q. The isotac v_1 through the point P' in the overlay represents $v_1 = v_s/q$.

Next we read the pressure tendency $(\partial p/\partial t)_1$ in the point $(x + \frac{1}{4}\frac{a_4}{a_3}\delta_3, y + \frac{1}{4}\delta_3)$ and $(\partial p/\partial t)_2$ in the point $\left(x - \frac{1}{4}\frac{a_4}{a_3}\delta_3, y - \frac{1}{4}\delta_3\right)$.

Compute $v_i = \dfrac{2a_3 \sec\alpha}{\varrho f^2 \delta_3}\{(\partial p/\partial t)_1 - (\partial p/\partial t)_2\}$.

For this computation it is convenient to take δ_3 in such a way that $\dfrac{2a_3 \sec\alpha}{\varrho f^2 \delta_3}$ has an easy to handle value. Determine next $v_s + v_i$ using the velocity scale along the vertical axis. The wind speed can now be read from the isotac v_2 through the point P for which holds $v_2 = (v_s + v_i)/q$. In the case of an anticyclonic pressure pattern the wind speed can be determined likewise but now the relation between q and δ_2 for anticyclonic curved isobars has to be used. Fig. 9 shows how the wind speed has to be determined in an anticyclonic pressure distribution.

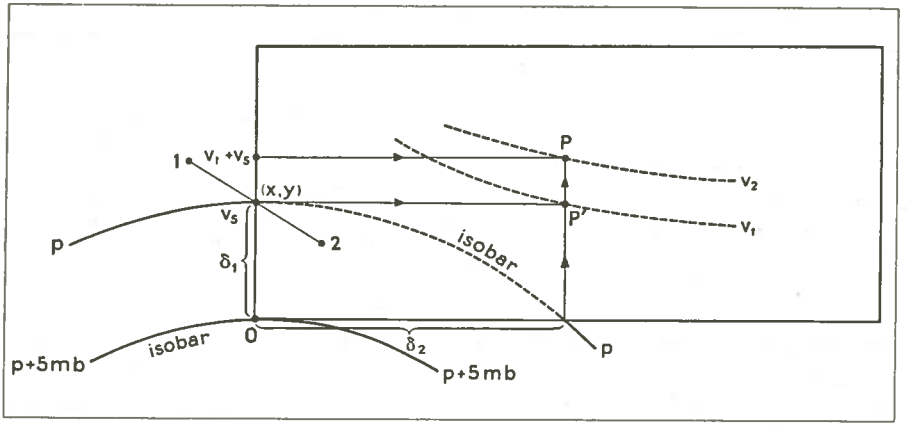

FIG. 9. Schematic representation of the relation between δ_2, v_s and v (------) and directions for the determination of the wind from a weather map (anticyclonic curvature of the isobars).

4.3 The overlay explained in the foregoing section only holds for a certain value of $T—T_s$, ϱ and φ, while difluence of the flow $(\partial G_y/\partial x)$ and geostrophic windshear $(\partial G_y/\partial y)$ are neglected. To account for stability it is necessary to have separate diagrams for different values of $T—T_s$. Fig. 10 shows a set of diagrams which has been constructed for the determination of the wind on the North Sea. For the computation of v_i the small figures in the left hand bottom corner of each diagram must be used. The difference $(\partial p/\partial t)_1 — (\partial p/\partial t)_2$ expressed in mb/3 hours and multiplied by 4 gives v_i in knots. The diagrams have been constructed for $\varrho = 1{,}25 \times 10^{-3}$ cm/g and for $\varphi = 55°$ ($f = 1{,}2 \times 10^{-4}$ sec^{-1}).

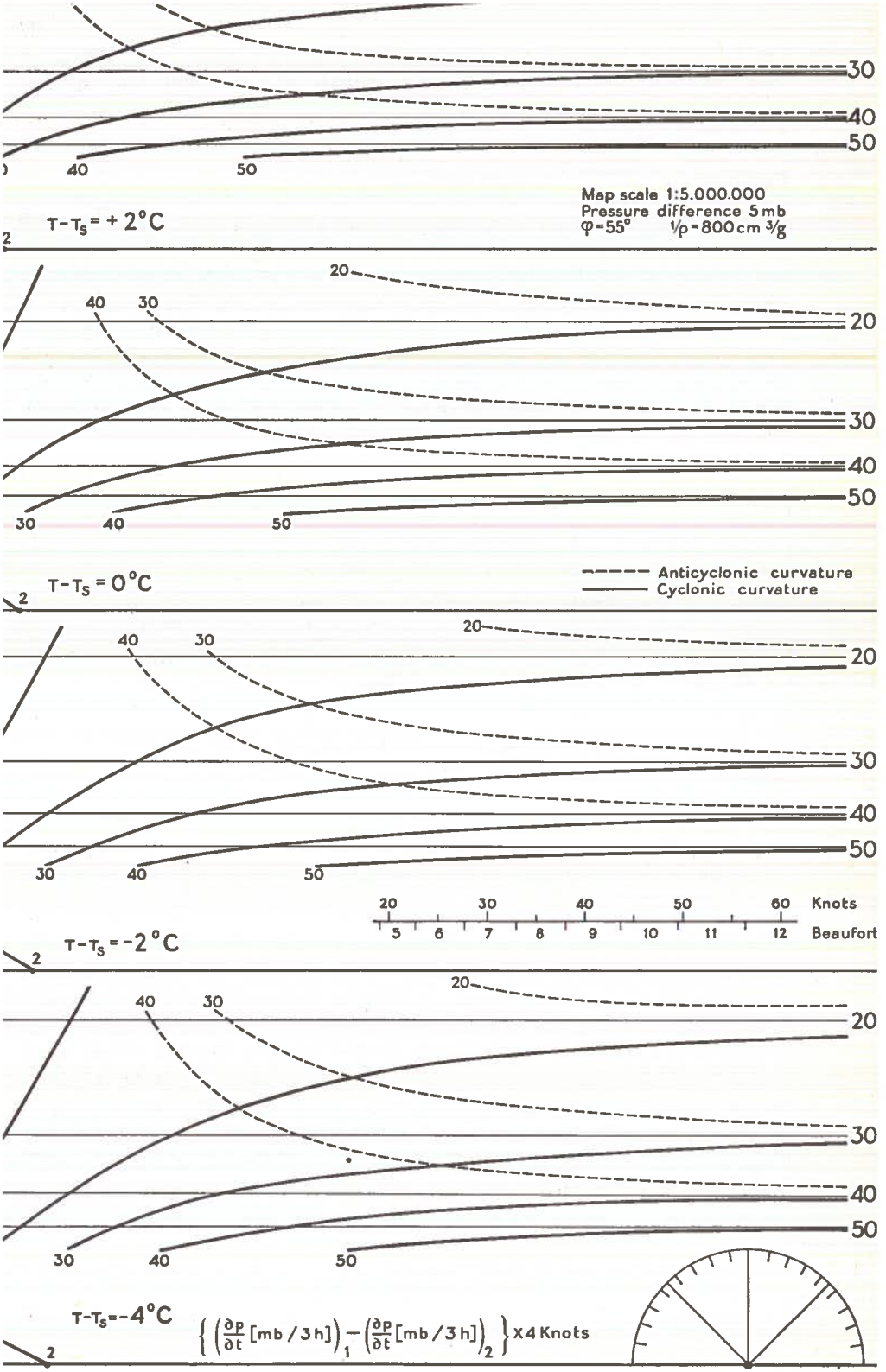
Map scale 1:5.000.000
Pressure difference 5 mb
φ=55° 1/ρ=800 cm³/g
T-Ts = + 2°C
T-Ts = 0°C
T-Ts = -2°C
T-Ts = -4°C
Anticyclonic curvature
Cyclonic curvature
20
30
40
50
60
Knots
5
6
7
8
9
10
11
12
Beaufort
{ (∂p/∂t [mb/3h])1 − (∂p/∂t [mb/3h])2 } x 4 Knots

When ϱ and f deviate from these standard values the diagrams consequently give incorrect wind velocities. The errors remain below 10 % between 50 and 60 degrees latitude (with the exception of extreme weather conditions of very high sea level pressure and very low temperature). If however corrections for the deviations of φ and ϱ from the standard values are required one can proceed as follows. Instead of using the diagram for the correct value of $T—T_s$ the wind speed has to be determined with a diagram holding for a smaller or greater value of $T—T_s$ according to the indications given in fig. 11. This method is based on the substitution of a_1 by $a_1^* = a_1 \frac{\varrho f}{\varrho_s f_s}$ (see Eq. (30)) and of a_4 by $a_4^* \approx a_4 \frac{\varrho f^2}{\varrho_s f_s}$ (see Eq. (31)) where ϱ_s and f_s denote the standard values. The use of fig. 11a reduces the errors due to deviating values of φ and ϱ from the standard values to less than about 3 %.

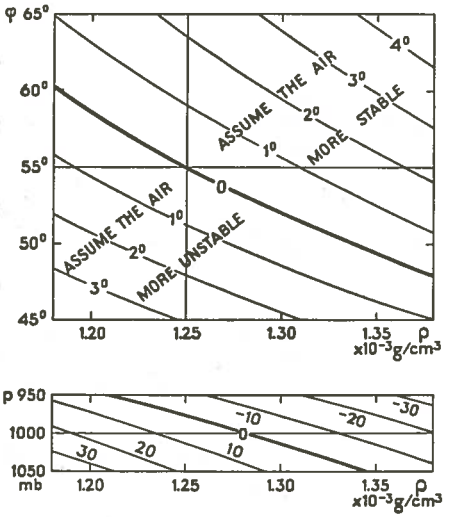

FIG. 11.

a. Diagram showing how to determine the wind speed with the overlay represented in fig. 10 when φ and ϱ deviate from the standard values.

b. The relation between T, p and ϱ; —— isotherms.

It remains now to correct for horizontal geostrophic windshear ($\partial G_y/\partial y \neq 0$) and difluent pressure patterns ($\partial G_y/\partial x \neq 0$). When there exists a considerable geostrophic windshear in the point (x, y) the wind speed must be determined by averaging the values obtained in the points $(x, y + \delta_1)$ and $(x, y - \delta_1)$. In the case of a strong difluent flow in (x, y) the best approximation can be obtained by taking δ_2 to the right (normal position of the overlay) if the flow is difluent and to the left (see fig. 12) if the flow is confluent. These manipulations are based on the experience obtained by the investigation with the pressure pattern models (section 3.5) that in a difluent or confluent flow Eq. (18)

gives higher wind velocities in comparison with pressure patterns showing the same gradient but equidistant isobars (see also table 4). Measuring the wind with the overlay in a confluent or difluent flow as mentioned above we take δ_2 too great with respect to Eq. (31) so that we obtain a higher wind speed and from experience just the right order of magnitude.

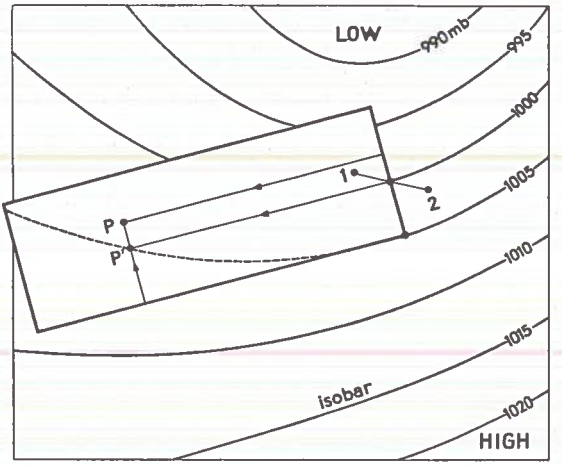

FIG. 12.
Direction for the use of the overlay in a confluent flow.

5. ON THE DETERMINATION OF THE PRESSURE TENDENCY FIELD

The application of the Eqs. (18) and (28) requires that the field of $\partial p/\partial t$ be known with a high degree of accuracy. For the investigation with the aid of pressure pattern models we could make use of the accessory pressure tendency fields. In practice the distribution of $\partial p/\partial t$ has mostly to be derived from weather reports. The synoptic reports of land stations and stationary ships give the pressure difference over 3 hours ($\Delta p/\Delta t$). In the reports of sailing ships $\Delta p/\Delta t$ refers to the pressure difference over 3 hours as measured on board.

For the determination of the wind in non-stationary pressure fields it appears in many cases that the approximation of $\partial p/\partial t$ by $\Delta p/\Delta t$ is insufficient. More accurate values can be derived from barograms but these records are seldom available. Another difficulty which arises when analysing the distribution of $\partial p/\partial t$ is the discontinuity in the $\partial p/\partial t$ field along front lines and trough axis. The approximation of $\partial p/\partial t$ by $\Delta p/\Delta t$ in the vicinity of fronts is unserviceable as may be seen from an example. Fig. 13 shows the distribution of $\Delta p/\Delta t$ belonging to model 3 represented by fig. 4.

Fig. 14 gives the differences between v/v_g computed with Eq. (28) using the field of $\partial p/\partial t$ as shown in fig. 4b and v/v_g computed with the same equation but using the field of $\Delta p/\Delta t$ represented by fig. 13 as an approximation for $\partial p/\partial t$. We see from fig. 14 that the errors introduced by using $\Delta p/\Delta t$ are considerably greater than the differences shown in the figs. 5, 6 and 7. It is evident that it is senseless to apply complicated relations between wind and non-stationary pressure distributions if the pressure tendency field is known with insufficient accuracy.

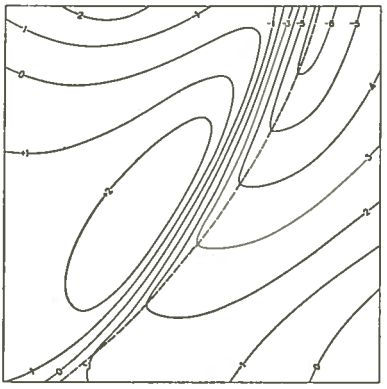

FIG. 13. Distribution of $\Delta p/\Delta t$ expressed in mb/3 hours (——) belonging to the model represented by fig. 4; ------- front.

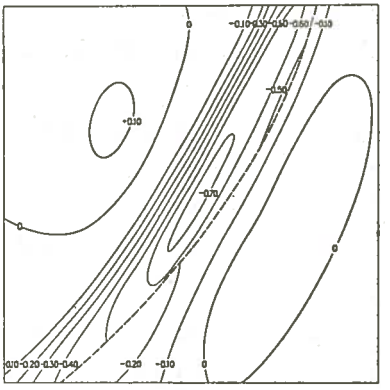

FIG. 14. Distribution of v/v_g computed with Eq. (28) using the field of $\partial p/\partial t$ represented by fig. 4a minus v/v_g computed with Eq. (28) using $\Delta p/\Delta t$ as shown by fig. 13.

6. CONCLUSION

A summary of the factors on which the wind at 10 m above the sea's surface depends is given in section 2.4. The advantage of the overlay developed in this contribution is that it enables directly to oversee the order of magnitude of the various factors for every separate case.

Some general rules for the determination of the surface wind over sea from weathermaps may be mentioned here.

1) When the isobars are little curved the stability of the air appears a very important factor.

2) When the isobars are strongly curved the stability can be neglected because in that case the curvature of the isobars becomes the dominating factor.

3) Only when the pressure tendency field is known very accurately it is justifiable to take into account the non-stationarity of a pressure system.

4) For forecasting it has in general no significance to account for shear, confluence or difluence and non-stationarity.

7. COORDINATE SYSTEM AND LIST OF SYMBOLS

In this contribution the earth's surface has been represented by a plain in which the location occurs by means of a right-angled coordinate system x, y. The height perpendicular to the earth's surface has been represented by z. The other symbols used have the following meaning:

A	„Austausch"coefficient
a_1, a_2, a_3, a_4	coefficients
$\vec{C}$	vector indicating the motion of a pressure system
C	$= \lvert \vec{C} \rvert$
C_x	x component of $\vec{C}$
c	friction factor
f	$= 2\,\omega \sin \varphi$
$\vec{G}$	$= \varrho^{-1}$ grad p (grad p = horizontal pressure gradient)
G	$= \lvert \vec{G} \rvert$
G_x, G_y	x and y component of $\vec{G}$
$\vec{k}$	unit vector perpendicular to the earth's surface
p	pressure
R	friction force
R	$= \lvert \vec{R} \rvert$
r	radius of curvature of the trajectory of a moving air particle (anticyclonic curvature $r > 0$; cyclonic curvature $r < 0$)
r_t	radius of curvature of an isobar
s	appendix indicating a standard value
T	air temperature
T_s	temperature of the sea's surface
t	time
$\vec{v}$	horizontal wind vector
v	$= \lvert \vec{v} \rvert$
v_x, v_y	x and y component of $\vec{v}$
$\vec{v}_g$	geostrophic wind vector ($\vec{v}_g = f^{-1}\,\vec{G} \times \vec{k}$)
v_g	$= \lvert \vec{v}_g \rvert$
$\vec{v}_{gr}$	gradient wind vector
v_{gr}	$= \lvert \vec{v}_{gr} \rvert$

$\vec{v}'$	vector difference between the wind in a stationary and a non-stationary pressure distribution
v_l	$= \lvert \vec{v}' \rvert$ if the isobars are straight and equidistant
v_s	$= v$ if the isobars are straight and equidistant and the pressure distribution stationary
α	angle between $\vec{v}$ and $\vec{v}_g$
β	angle between $\vec{R}$ and $-\vec{v}$
$\varkappa$	friction coefficient
λ	$= \sqrt{\frac{f\varrho}{2\lambda}}$
ϱ	air density
φ	latitude
ψ	angle between $\vec{c}$ and $\vec{v}_g$
ω	the angular velocity of the earth's rotation

ACKNOWLEDGEMENT

The author wishes to thank Dr. F. H. SCHMIDT for his advices and helpful criticism concerning the present study.

SUMMARY

A relation between the surface wind over sea and stationary and non-stationary pressure distributions has been derived with the aid of publications of HESSELBERG and SVERDRUP and empirical data collected by BLEEKER and VERPLOEGH. A slight simplification of the formula makes it possible to construct a simple overlay for the determination of the surface wind over sea from the isobar patterns on weather maps.

REFERENCES

1. BAUR, F. und PHILIPPS, H. 1938 Untersuchung der Reibung bei Luftströmungen über dem Meer. Ann. d. Hyd. **60**, 291.
2. BLEEKER, W. 1940 Berekening wrijvingsfactor boven zee. K.N.M.I. Intern verslag.
3. BLEEKER, W. 1942 Leerboek der Meteorologie I, Zutphen, W. J. Thieme & Cie, 39–40.
4. BRUNT, D. and DOUGLAS, C. K. M. 1928 Modification of the geostrofic balance. Mem. Roy. Met. Soc. **3**, 29–33.
5. HESSELBERG, T. 1915 Ueber eine Beziehung zwischen Druckgradient, Wind und Gradientänderungen. Veröffentl. d. Geoph. Inst. Leipzig, Serie 2, Band 1, 207–210.
6. HESSELBERG, T. und SVERDRUP, H. U. 1915 Die Reibung in der Atmosphäre. Veröffentl. d. Geoph. Inst. Leipzig, Serie 2, Band 1.
7. KOSCHMIEDER, H. 1950 Dynamische Meteorologie. 3e Auflage, Leipzig, Akademische Verlagsgesellschaft, 286–294.
8. PETTERSSEN, S. 1940 Weather analysis and forecasting. New York/London, MCGRAW-HILL Book Company, 225.
9. PHILIPPS, H. 1939 Die Abweichung vom Geostrophischen Wind. Met. Z., **56**, 468.
10. POSTMA, K. R. 1948 The formation and development of occluding cyclones. K.N.M.I. Med. en Verh., Serie B, deel 10, 15.
11. VERPLOEGH, G. 1954 Enige bepalingen van de wrijvingscoëfficient boven zee (nog te publiceren rapport).
12. VERPLOEGH, G. 1955 De gemiddelde afwijkingshoek van de grondwind boven zee t.o.v. de geostrophische windrichting. K.N.M.I., Korte Mededeling, IV–1.